A Simple Review of EEG Foundation Models: Datasets, Advancements and Future Perspectives

Junhong Lai[1,2,3], Jiyu Wei[1,2,3] , Lin Yao[1,2,3] and Yueming Wang[1,2,3,4]

[1]The College of Computer Science, Zhejiang University, Hangzhou, China.
[2]The MOE Frontiers Science Center for Brain and Brain-Machine Integration, Zhejiang University, Hangzhou, China.
[3]The Nanhu Brain-Computer Interface Institute, Hangzhou, China.
[4]The Qiushi Academy for Advanced Studies, Hangzhou, China.

Electroencephalogram (EEG) signals play a crucial role in understanding brain activity and diagnosing neurological diseases. Because supervised EEG encoders are unable to learn robust EEG patterns and rely too heavily on expensive signal annotation, research has turned to general-purpose self-supervised EEG encoders, known as EEG-based models (EEG-FMs), to achieve robust and scalable EEG feature extraction. However, the readiness of early EEG-FMs for practical applications and the standards for long-term research progress remain unclear. Therefore, a systematic and comprehensive review of first-generation EEG-FMs is necessary to understand their current state-of-the-art and identify key directions for future EEG-FMs. To this end, this study reviews 14 early EEG-FMs and provides a critical comprehensive analysis of their methodologies, empirical findings, and unaddressed research gaps. This review focuses on the latest developments in EEG-based models (EEG-FMs), which have shown great potential for processing and analyzing EEG data. We discuss various EEG-FMs, including their architectures, pretraining strategies, pretraining and downstream datasets, and other details. This review also highlights challenges and future directions in the field, aiming to provide a comprehensive overview for researchers and practitioners interested in EEG analysis and related EEG-FM.

Index Terms—Electroencephalogram (EEG), EEG foundation model(EEG-FM).

I. INTRODUCTION

EEG is a non-invasive technique that records the electrical activity of the brain. It has been widely used in neuroscience research, clinical diagnosis, and brain-computer interfaces (BCIs) [1]. However, EEG data analysis is challenging due to its low signal-to-noise ratio (SNR), high dimensionality, non-stationarity, and individual variability [2], [3]. As highly objective physiological signals, EEG has demonstrated remarkable potential in seizure epilepsy classification [4], acute stress detection [5], sleep stage classification [6], motor imagery recognition [7], abnormal identification [8], emotion analysis [9], and auditory attention detection [10].

Although EEG modeling has attracted extensive research attention, several issues remain unresolved. Currently, research on EEG recording modeling is mainly divided into two research lines, including manual feature methods [11] and deep learning-based methods [12]. Manual feature engineering requires a lot of domain knowledge and may only be applicable to specific tasks. In addition, most deep learning-based methods are fully supervised, which heavily relies on labeled data. However, large-scale labeled data is often infeasible or expensive in medical experiments, highlighting the importance of maximizing labeling efficiency.

In recent years, the emergence of large-scale pre-training models has revolutionized the field of natural language processing(LLM) [13], [14] and computer vision(VLM) [15]–[17]. Inspired by these successes, researchers have started to explore the application of large models in EEG analysis [18]. These models can learn hierarchical representations from large amounts of unlabeled EEG data, which can then be fine-tuned for specific tasks, such as seizure detection, emotion recognition, and cognitive state assessment. This approach has the potential to improve the performance and generalization ability of EEG analysis models, while reducing the need for labeled data [19].

Motivated by the potential of EEG-FMs(EEG Foundation Models) and an increasing number of recent papers proposing EEG-FMs for various EEG tasks, there is an urgent need for a comprehensive review of EEG-FMs for EEG applications. The main contributions of this paper include:

- Summarizing the overview of different EEG-FMs.
- Summarizing the datasets for pre-training and downstream of EEG-FMs.
- Summarizing the details for pre-training and evaluation of EEG-FMs.
- Future perspectives for EEG-FMs.

By addressing these essential aspects, this review paper will provide a comprehensive and in-depth analysis of the application of EEG-FMs for EEG tasks. The goal of this review is to provide a comprehensive overview of the current state-of-the-art EEG foundation models. The models we investigated include the following: Brant [19][1], BrainWave(Brant-2) [20][2], LaBraM [21][3], NeuroGPT [22][4], BIOT [23][5], EEGPT1 [24][6], BrainBERT [25][7], FoME [26][8], EEGPT2 [27], MBrain [28],

---

[1]https://zju-brainnet.github.io/Brant.github.io/
[2]https://github.com/yzz673/Brant-2
[3]https://github.com/935963004/LaBraM
[4]https://github.com/wenhui0206/NeuroGPT
[5]https://github.com/ycq091044/BIOT
[6]https://github.com/BINE022/EEGPT
[7]https://github.com/czlwang/BrainBERT
[8]https://github.com/1061413241/FoME

NeuroLM [29], CBraMod [30][9], EEGFormer [31] and ALFEE [32][10].

We will discuss the key techniques and architectures used in these models, their performance on various tasks, and the challenges and future directions in this field. By summarizing the latest research findings, we hope to promote further research and development in EEG foundation models and facilitate their application in clinical and research settings.

II. Overview of EEG Foundation Models

EEG-FMs have emerged as a powerful tool in the analysis and interpretation of EEG signals, leveraging large-scale data and unsupervised training approaches, similar to other large models like those used in NLP fields. These models aim to capture complex temporal and spatial dependencies in EEG data, which can be utilized for tasks such as classification, prediction, and anomaly detection. EEG-FMs have gained significant attention due to their ability to model intricate patterns in brain activity, with applications in clinical diagnostics, cognitive neuroscience, BCIs, and more. EEG-FMs typically undergo unsupervised pretraining using vast datasets, allowing the model to learn relevant features and representations from EEG signals without the need for extensive labeled data.

In EEG-related tasks, the input consists of multichannel EEG recordings, where each channel corresponds to a node, and the connectivity between channels (based on functional or structural relationships) represents edges in the model. The data is typically time-series, meaning each EEG signal consists of a series of voltage readings sampled over time, often captured from multiple electrodes placed on the scalp. A large model learns to extract patterns from these signals, and the objective is to predict or classify brain states, such as detecting epileptic seizures, identifying cognitive states, or differentiating between disorders like ADHD or Alzheimer's disease.

Compared to traditional machine learning models, EEG-FMs offer several advantages. First, like other large models, they are capable of learning representations directly from raw EEG data, which bypasses the need for manual feature extraction. This ability to handle complex, high-dimensional data makes them particularly powerful for EEG analysis, as they can learn both temporal and spatial patterns from the raw signal. EEG-FMs are also designed to handle the large-scale and diverse nature of EEG data, which may come from different subjects, tasks, and experimental conditions, making them highly versatile and robust. Furthermore, similar to other deep learning models, EEG-FMs can learn hierarchical representations, capturing both low-level features (e.g., oscillatory patterns) and high-level brain network dynamics, leading to improved performance on a variety of tasks. Several advanced techniques in EEG-FMs, such as transformers and self-supervised learning, allow the model to leverage vast amounts of unlabelled EEG data for pretraining, significantly improving generalization to new, unseen data.

The architecture of EEG-FMs varies depending on the task, but common approaches mainly include convolutional neural networks (CNNs) and transformers. These models are typically designed to process the temporal aspect of EEG signals (e.g., using CNNs) as well as the spatial relationships between electrodes (e.g., using attention mechanisms). In particular, transformer models, which have been successful in natural language processing, have been adapted to handle EEG data by processing long-term temporal dependencies and capturing complex spatial relationships between EEG channels. The large-scale nature of EEG-FMs enables them to generalize across different subjects and experimental conditions, making them suitable for a wide range of applications, including brain-computer interfaces (BCIs), cognitive state monitoring, and clinical diagnostics.

EEG-FMs are trained on vast amounts of EEG data from multiple sources, ensuring that the model learns the underlying patterns that are consistent across different individuals and experimental conditions. By using unsupervised learning techniques, such as contrastive learning or self-supervised learning, EEG-FMs can efficiently learn from large datasets without requiring manual labeling, which is often a significant challenge in EEG research. The ability to scale up to large datasets also allows EEG-FMs to adapt to diverse applications, from medical diagnosis to real-time brain-state monitoring in brain-computer interfaces.

A. Data collection and preprocessing

Large language model pretraining usually requires a lot of data, and so does the EEG foundation model. Therefore, the first step in pretraining a large model is usually to collect as many EEG datasets as possible to ensure that the diversity and representativeness of the pretraining dataset can fully ensure that the model can fully learn the various characteristics of brain activity.

EEG data usually has a low SNR, and the preprocessing of the data usually includes: bandpass filtering, notch filtering, resampling and normalization. Generally speaking, there is no need to use ICA for additional artifact removal. We discuss the preprocessing steps of each EEG-FM in detail in Section.III-B.

- **Bandpass filtering**. Bandpass filter the EEG signal to remove low-frequency noise (e.g. 0.1 Hz - 75 Hz).
- **Notch filtering**. Apply a notch filter to avoid power line interference (e.g. 50 Hz).
- **Resampling**. Resample all EEG signals (e.g. 200hz).
- **Normalization**. Normalize the EEG signal (e.g., z-score).

B. Model architecture

In this section, we detail the whole framework of universal EEG-FM, though their model architecture details and pretraining details may not be exactly the same. The Overview of the architecture and workflow of general EEG-FM is illustrated in Fig.1. We can formulate the multi-channel EEG signals as $X \in \mathbb{R}^{T \times C}$, where C is the number of EEG channels and T is the total timestamps.

---

[9]https://github.com/wjq-learning/CBraMod
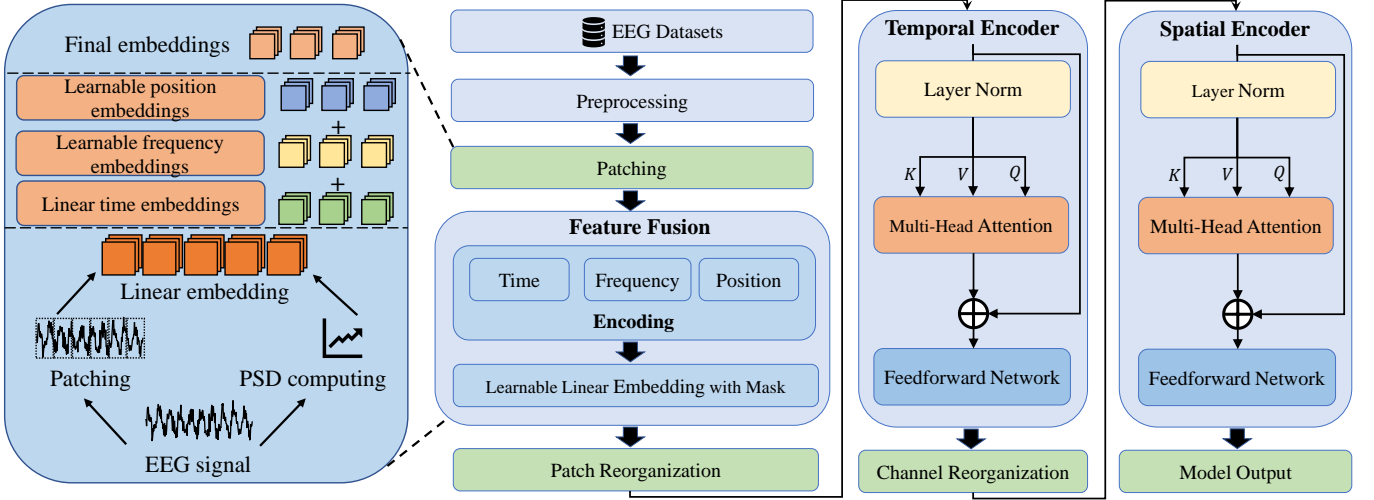[10]https://github.com/xw1216/ALFEE

Fig. 1: Overview of the architecture and workflow of general EEG-FM.

1) Patching

Since neural recordings are electrical signals with high sampling rates, we aggregate timestamps into patches to (1) enhance the locality and extract semantic information; (2) reduce computation and memory usage; and (3) attend a longer temporal dependency [33]. Assume that the timestamp for each sample is t and the stride is s. X can be segmented into $\lfloor \frac{T-t}{s} + 1 \rfloor$, and each sample $x \in \mathbb{R}^{t \times C}$, where t is the number of timestamps and C is the number of electrode channels, we divide x with length M, stride S and overlap O, where $O = M - S$ is the number of overlapping timestamps between consecutive patches. This generate a set of patches $p \in \mathbb{R}^{N_p \times C \times M}$, where $N_p = \lfloor \frac{t-M}{S} + 1 \rfloor$ is the number of patches in each channel. In fact, p can be represent as:

$$\left\{ p_{k,c} \in \mathbb{R}^M \mid k = 1, 2, ..., \left\lfloor \frac{t-M}{S} + 1 \right\rfloor; c = 1, 2, ..., C \right\}$$ (1)

2) Time-Encoding

The time-encoding is composed of a linear projection layer. Specifically, the input $p \in \mathbb{R}^{N_p \times C \times M}$ contains $N_p \times C$ patches with length M and $p_c \in \mathbb{R}^{N_p \times M}$ denotes the patches in c-th channel. We map each sequence of patches $p_c \in \mathbb{R}^{N_p \times M}$ to the latent space of dimension D by a linear projection $W_{proj} \in \mathbb{R}^{M \times D}$, which can be presented as $e_c = (W_{proj}^T p_c)^T$. We denote the time-encoding embeddings as $e \in \mathbb{R}^{N_p \times C \times D}$:

3) Frequency-Encoding

The frequency-encoding mainly extracts the power density value corresponding to each frequency and calculated the power sum within the frequency band according to the preset n frequency band intervals $[f_{min}, f_{max}]$, where $0 < f_{min} < f_{max} < f_{Nyquist}$ [34]. For EEG signals, we usually divide the frequency spectrum into five bands: δ (1-4Hz), θ (48Hz), α (8-13Hz), β (13-30Hz), γ (30-50Hz). For the i-th frequency band, a learnable encoding $f_i \in \mathbb{R}^{N_p \times D}$ is set as its representation which is shared across all the patches. For a given patch $P_{k,c}(t) = p_{k,c}$, we first apply the Fourier transform [35] to

convert the time-domain signal into the frequency domain. The power spectral density(PSD), denoted as $P_{k,c}(f)$, is then calculated by squaring the magnitude of the frequency components:

$$P_{k,c}(f) = \frac{1}{T} |\mathcal{F}\{P_{k,c}(t)\}|^2 = \frac{1}{T} \left| \int_{-\infty}^{\infty} P_{k,c}(t) e^{-i2\pi ft} dt \right|^2$$ (2)

where f is the frequency, T is the total duration of the signal segment, and $\mathcal{F}$ is the Fourier transform. Subsequently, we compute the sum of power within each sub-band $[f_{min}, f_{max}]$:

$$PSD_{k,c}(i) = \log_{10}\left(\sum_{f_i = f_{min}}^{f_{max}} P_{k,c}(f) + 1 \right)$$ (3)

$PSD_{k,c}(i)$ acts as the weight of f_i. The frequency encoding $F_{k,c} \in \mathbb{R}^D$ of patch $p_{k,c}$ is obtained as the weighted sum of the learnable encodings f_i:

$$F_{k,c} = \sum_{i=1}^{|\text{bands}|} \frac{\exp(P_{k,c}(i))}{\sum_{i'=1}^{|\text{bands}|} \exp(P_{k,c}(i'))} f_i$$ (4)

4) Position-Encoding

A learnable positional encoding $W_{c,pos} \in \mathbb{R}^{N_p \times D}$ monitors the temporal order of patches $p_c \in \mathbb{R}^{N_p \times M}$.

5) Time-Frequency Fusion

According to the previous steps, we can obtain the time-encoding $e \in \mathbb{R}^{N_p \times C \times D}$, frequency-encoding $F \in \mathbb{R}^{N_p \times C \times D}$, position-encoding $W_{pos} \in \mathbb{R}^{N_p \times C \times D}$. We can obtain the fusion-encoding $\tilde{p} \in \mathbb{R}^{N_p \times C \times D}$ by adding them together:

$$\tilde{p} = e + F + W_{pos}$$ (5)

6) Temporal Encoder

The Temporal Encoder is designed to capture long-range dependencies and intricate temporal patterns within EEG data, which consists of a stack of dense Transformer encoding

layers. Each layer encompasses three key modules: multi-head self-attention, feedforward neural network, and layer normalization with residual connections. Given an input embedding $\tilde{p} \in \mathbb{R}^{N_p \times C \times D}$ obtained from the previous step, we apply a trainable linear transformation along the temporal dimension to derive the query, key, and value matrices for the attention operation, denoted as $Q_{time}^i, K_{time}^i, V_{time}^i \in \mathbb{R}^{N_p \times D}$ respectively. The temporal dependencies are then modeled by computing the attention score $\text{Attention}_{time}^i$:

$$\text{Attention}_{time}^i = \text{Softmax}(Q_{time}^i (K_{time}^i)^T / \sqrt{D}) V_{time}^i \quad (6)$$

In the multi-head self-attention mechanism, the query, key, and value matrices are linearly projected into D_k, D_k, D_v. Subsequently, the attention function is applied to each projected version, yielding an output of dimension D_v. These outputs are concatenated and mapped back to the original dimension D to obtain the final attention value:

$$\text{MultiHead}(Q, K, V) = \text{Concat}(head_1, ..., head_h)W^O \quad (7)$$

where $head_i = \text{Attention}(QW_i^Q, KW_i^K, VW_i^V), W_i^Q \in \mathbb{R}^{D \times D_k}, W_i^K \in \mathbb{R}^{D \times D_k}, W_i^V \in \mathbb{R}^{D \times D_v}$, and $W^O \in \mathbb{R}^{D \times hD_v}$ denote the projection matrix. Finally get the output $\hat{p} \in \mathbb{R}^{N_p \times C \times D}$.

7) Spatial Encoder

The Spatial Encoder is specifically designed to capture spatial relationships and inter-channel dynamics within EEG data. Recognizing the intricate interactions between different brain regions represented by distinct EEG channels, this encoder adapts to learn channel-specific characteristics and their interdependencies. Similarly, given an input embedding $\hat{p} \in \mathbb{R}^{N_p \times C \times D}$ obtained from the previous step, we apply a trainable linear transformation along the channel dimension to derive the query, key, and value matrices for the attention operation, denoted as $Q_{ch}^i, K_{ch}^i, V_{ch}^i \in \mathbb{R}^{N_p \times D}$ respectively. Finally, we compute the attention score Attention_{ch}^i, which involves the interactions between channels and represents the spatial dynamics of the brain:

$$\text{Attention}_{ch}^i = \text{Softmax}(Q_{ch}^i (K_{ch}^i)^T / \sqrt{D}) V_{ch}^i \quad (8)$$

The application of multi-head self-attention mechanism in this part is similar to the previous part. Finally get the output $\bar{p} \in \mathbb{R}^{N_p \times C \times D}$.

C. Reconstruction

Constructing the reconstruction loss allows the model to learn the potential representation of EEG data and the spatio-temporal and frequency domain characteristics of EEG data on unlabeled data through self-supervised learning tasks, thereby improving the model's adaptability to noise and occlusion. The overview of neural tokenizer training and EEG-FM pre-training is illustrated in Fig.2.

The existing model mainly includes the following four types of reconstruction objectives(see Tab.VIII): original patches, potential representation of patches(embeddings), frequency domain features of patches, and codebook prediction.

1) Reconstruction of original patches

During the pre-training stage, the representations $\bar{p} \in \mathbb{R}^{N_p \times C \times D}$ will be fed into a flatten layer with linear head $W_{rec} \in \mathbb{R}^{D \times M}$ to reconstruct the original patches $\check{p} \in \mathbb{R}^{N_p \times C \times M}$. Finally we utilize an MSE loss to measure the discrepancy between the reconstructed patches and the original patches:

$$\mathcal{L}_{op} = \frac{1}{N_p} \sum_i^{N_p} ||p_i - \check{p}_i||_2^2 \quad (9)$$

where $\check{p}_i, p_i \in \mathbb{R}^{\times C \times M}$, $i = 1, 2, \ldots, N_p$.

2) Reconstruction of patches embeddings

We utilize an MSE loss to measure the discrepancy between the reconstructed patches embeddings $\tilde{e} \in \mathbb{R}^{N_p \times C \times D}$ and the patches embeddings $\tilde{p} \in \mathbb{R}^{N_p \times C \times D}$:

$$\mathcal{L}_{pe} = \frac{1}{N_p} \sum_i^{N_p} ||\tilde{e}_i - \tilde{p}_i||_2^2 \quad (10)$$

where $\tilde{p}_i, \tilde{e}_i \in \mathbb{R}^{\times C \times D}$, $i = 1, 2, \ldots, N_p$.

3) Reconstruction of fourier spectrum

For an EEG patch $p_{k,c} = [p[1], p[2], ..., p[N_p]]$ of channel c and time k in a sample p, we apply the Discrete Fourier Transform (DFT) as follows:

$$\widetilde{p}_{c,k}^m = \sum_{n=1}^{N_p} p[n] \exp\left(-\frac{2\pi j}{N_p} mn\right) \quad (11)$$

where $m \in [1, N_p]$ and j is the imaginary unit. We rewrite Equation 11 using Euler's formula as:

$$\widetilde{p}_{c,k}^m = \sum_{n=1}^{N_p} p[n] \cos\left(\frac{2\pi}{N_p} mn\right) - jp[n] \sin\left(\frac{2\pi}{N_p} mn\right) \quad (12)$$

where $\widetilde{p}_{c,k}^m$ indicates the spectrum of the sequence at frequency $\omega_m = \frac{2\pi m}{N_p}$. The the amplitude and phase can be calculated as:

$$\begin{cases} A^m = \sqrt{\text{Re}\left(\widetilde{p}_{c,k}^m\right)^2 + \text{Im}\left(\widetilde{p}_{c,k}^m\right)^2} \\ \phi^m = \arctan\left(\frac{\text{Im}(\widetilde{p}_{c,k}^m)}{\text{Re}(\widetilde{p}_{c,k}^m)}\right) \end{cases} \quad (13)$$

where Re and Im represent the real and imaginary parts of a complex number. We usually apply z-score normalization to normalize A^m and ϕ^m within a sample for stable convergence.

The output representations are aggregated by average pooling followed by two specific prediction heads to regress the spectrum amplitude o^A and phase o^ϕ, respectively. The mean squared error (MSE) loss is utilized to guide the prediction:

$$\mathcal{L}_A = \frac{1}{N_p} \sum_{i=1}^{N_p} \left\| o_i^\phi - \phi_i \right\|_2^2 \quad (14)$$

$$\mathcal{L}_\phi = \frac{1}{N_p} \sum_{i=1}^{N_p} \left\| o_i^\phi - \phi_i \right\|_2^2 \quad (15)$$
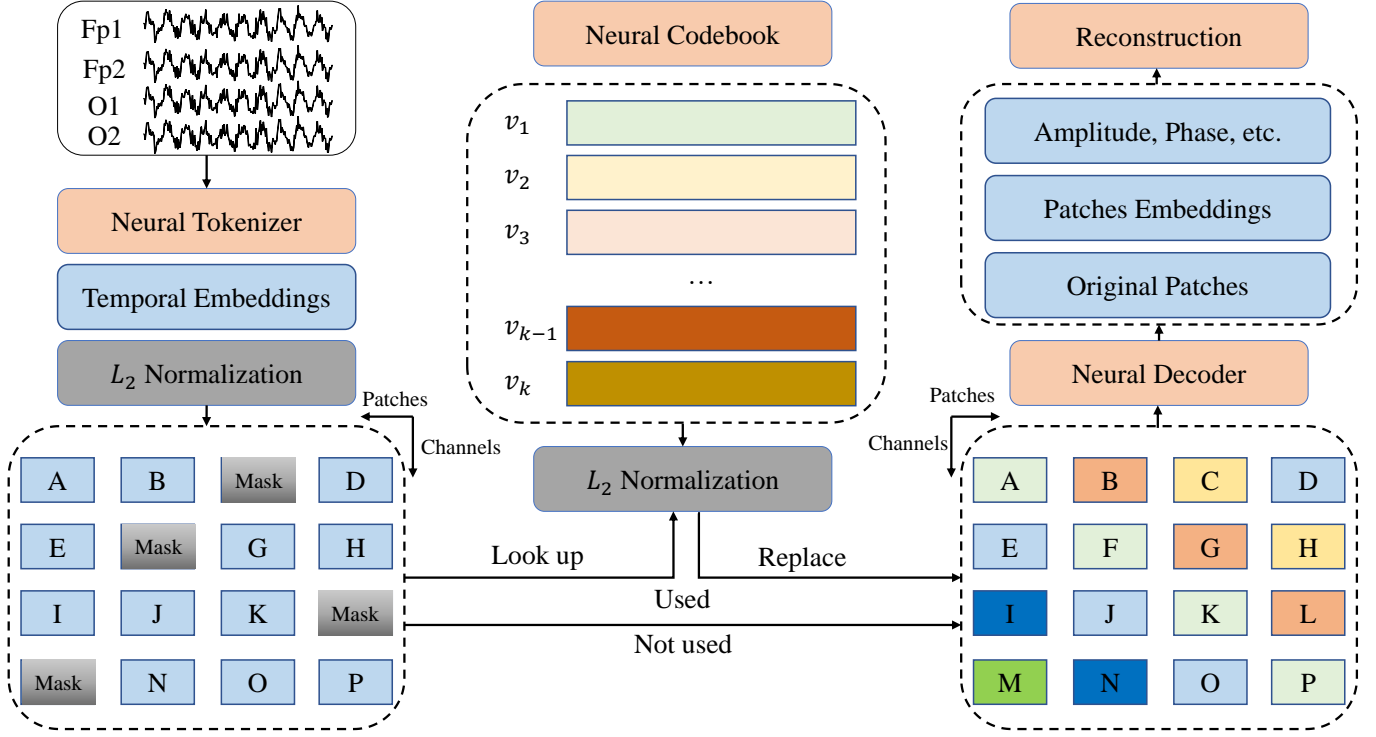
Fig. 2: Overview of neural tokenizer training and EEG-FM pre-training.

4) Codebook prediction

Codebook prediction consists of two parts:Neural tokenizer training and embedding prediction.

For **Neural Tokenizer Training**: We define a neural codebook $\mathcal{V} = \{v_i \mid i = 1, \ldots, K\} \in \mathbb{R}^{K \times D}$, where K is the number of the discrete neural embeddings and D is the dimensionality of each embedding. All time-encoding embeddings $e \in \mathbb{R}^{N_p \times C \times D}$ are stored in the codebook $\mathcal{V}$. We utilize a quantizer to quantize all the patch representations into the neural codebook embeddings. The codebook looks up the nearest neighbor of each patch p_i in the neural codebook $\mathcal{V}$. This procedure can be formulated as:

$$z_i = \arg\min_j \|\ell_2(p_i) - \ell_2(v_i)\|_2, \tag{16}$$

where ℓ_2 represents ℓ_2 normalization and z_i is the quantized vector after the quantizer. This is equivalent to finding the closest neural embedding by cosine similarity and such ℓ_2 normalization improves the codebook utilization [36].

$$\mathcal{L}_{ntt} = \frac{1}{N_p}\sum_i^{N_p} \left\|\mathbf{sg}\left(\ell_2\left(p_i\right)\right) - \ell_2\left(v_{z_i}\right)\right\|_2^2 + \left\|\ell_2\left(p_i\right) - \mathbf{sg}\left(\ell_2\left(v_{z_i}\right)\right)\right\|_2^2 \tag{17}$$

where sg represents the stop-gradient operation that is defined as an identity at the forward pass and has zero gradients. For **Embedding prediction**: We randomly generate a mask $\mathcal{M} = \{m_i \in \{0, 1\} \mid i = 1, \ldots, N_p\}$. After that, we replace the masked patches of p with the learnable mask token $e_\mathcal{M} \in \mathbb{R}^D$. The corrupted EEG patches can be denoted as $e^\mathcal{M} = \{e_i : m_i = 0 | i = 1, 2, \ldots, N_p\} \cup \{e_\mathcal{M} : m_i = 1 | i = 1, 2, \ldots, N_p\}$. , which will be added by

subsequent modules. $\bar{\boldsymbol{p}} \in \mathbb{R}^{N_p \times C \times D}$ are used to predict the corresponding neural tokens through a linear classifier:

$$p(\boldsymbol{v}' | \boldsymbol{e}^\mathcal{M}) = \text{softmax}(\text{Linear}(\bar{\boldsymbol{p}})) \tag{18}$$

The linear layer outputs a vector $o_i \in \mathbb{R}^\mathcal{V}$ of length $\mathcal{V}$, where each element $o_{i,j}$ represents the unnormalized probability that the patch is predicted to be the j-th token in the Codebook. The Softmax function converts the unnormalized probability into a probability distribution.

$$p(v'_j \mid e^\mathcal{M}) = \frac{\exp(o_{i,j})}{\sum_{k=1}^V \exp(o_{i,k})}, \quad j = 1, 2, \ldots, V \tag{19}$$

where $p(\boldsymbol{v}' | \boldsymbol{e}^\mathcal{M})$ is the probability that the model predicts that the token corresponding to $\bar{p}_i$ is v_j.

The objective training loss is:

$$\mathcal{L}_{eq} = -\sum_{m_i=1} \log p(v_i | \boldsymbol{e}^\mathcal{M}) \tag{20}$$

III. SURVEY RESULTS

This survey is based on a review of 11 articles. These articles were selected by title and abstract screening from a search on Google Scholar and ScienceDirect queried on December 9st, 2024. The search query for collecting the articles was defined as: ("LLM" OR "Foundation model") AND ("Electroencephalography" OR "EEG"). Both peer-reviewed articles and preprints were included. All types of EEG foundation model were included.

In the remaining portion of this paper, we report the categories of comparisons we identified in the surveyed papers. These are based on the different aspects of the proposed EEG-based LMs. Specifically, these are:

- Datasets for pretraining and downstream tasks.
- Preprocessing conditions of datasets.
- The evaluation methods of EEG-FMs.
- The parameter size of EEG-FMs.
- The objective loss function of EEG-FMs.
- The hardware conditions for pre-training of EEG-FMs.

The following parts will provide further details on these aspects, and the paper will conclude by discussing trends and proposing plausible directions for future research.

A. Pretraining and Downstream Datasets

In the pre-training of EEG foundation models, the diversity and representativeness of dataset are crucial. In order to ensure that the model can fully learn the various characteristics of brain activity, a large amount of EEG signal data must be collected. For research teams with conditions, these data not only include public data sets, but can also be combined with self-collected data. Comprehensive data collection usually needs to take into account task diversity, subject diversity, diversity of collection conditions, and diversity of time spans and frequencies. Through comprehensive and diverse data collection, EEG foundation models can obtain richer training data, and then learn more universal and detailed features, thereby demonstrating better performance and generalization capabilities in practical applications. According to our statistics(see Tab.I), Brant-2 uses the most pre-training data, reaching 13.79TB, and the EEG recording time is about 40,000 hours.

TABLE I: The size and length of EEG datasets used to pre-train the model

Model	Size	Length
Brant [19]	1.01TB	2528h
Brant-2 [20]	13.79TB	40,907h
LaBraM [21]	-	about 2,500h
NeuroGPT [22]	-	5656h
BIOT [23]	-	-
EEGPT1 [24]	-	-
BrainBERT [25]	-	43.7h
FoME [26]	1.7TB	about 26,000h
EEGPT2 [27]	-	-
MBrain [28]	at least 550GB	at least 470h
NeuroLM [29]	-	about 25,000h
CBraMod [30]	-	27,062h
EEGFormer [31]	1.7TB	about 26,000h
ALFEE [32]	-	about 25,000h

- Indicates that the corresponding article does not explicitly mention the size or length of EEG datasets for pre-training.

In addition, to evaluate the performance of EEG foundation models in downstream tasks, it is necessary not only to use standard performance indicators, but also to pay attention to the model's generalization ability, interpretability, robustness, computational efficiency and other dimensions. Therefore, the selection of downstream task data also needs to take into account the relevance and complexity of the task. We have collected all relevant datasets for pre-training and downstream tasks for all the models, see the Tab.II Tab.III and Tab.IV. As can be seen from the table, different EEG-FMs utilize varying pre-training datasets and downstream task datasets, which can pose challenges. The size and quality of pre-training data can impact EEG-FM performance, making it difficult to objectively compare the best performance of different EEG-FMs on downstream tasks.

TABLE II: Datasets for pretraining and downstream tasks

	Pretraining Datasets	Downstream Datasets
Brant [19]	**	MAYO [37]
	-	FNUSA [37]
	-	**
Brant-2 [20]	CCEP [38]	AD-65 [39]
	CAP [40]	CHB-MIT [41]
	HMS [42]	Mayo-Clinic [37]
	Siena [43]	FNUSA [37]
	SRM [44]	MDD-64 [45]
	TUEG [46]	Depression-122 [47]
	Schizophrenia-81	Schizophrenia-28 [48]
	Sleep-EDF [49]	ADHD-Adult [50]
	Stroke-50 [51]	ADHD-Child [52]
	PD-31 [53]	SD-71 [54]
	IowaDataset	-
	UNMDataset	-
	AD-184 [55]	-
	**	-
LaBraM [21]	BCICIV-1 [56]	TUAB [57]
	Emobrain [58]	TUEV [57]
	Grasp and Lift [59]	SEED-V [60]
	Inria BCI [61]	MoBI [62]
	MMI [63]	-
	RAW [64]	-
	RSEEG [65]	-
	Siena [43]	-
	TVNT [66]	-
	TUAR [67]	-
	TUEP [68]	-
	TUSZ [57]	-
	TUSL [69]	-
	SEED [70]	-
	SEED-V [60]	-
	SEED-GER [71]	-
	Self-collected [72]–[76]	-
NeuroGPT [22]	TUH [57]	BCIC-2A [77]
BIOT [23]	SHHS [78], [79]	-
	PREST(*)	-
	Cardiology [80]	-
	CHB-MIT [41]	-
	IIIC-Seizure [81]	-
	TUAB [57]	-
	TUEV [57]	-
	PTBXL [82]	-
	HAR [83]	-

** Indicates the dataset may be private and the authors have not explicitly cited any literature in the paper.
* Indicates the corresponding dataset is private .
The data not cited any literature in the table are not mentioned in the corresponding article.

B. Datasets preprocessing

In the data preprocessing of EEG signals, denoising, artifact removal and standardization are generally required. If you consider using EEG signals as pre-training data, you generally need to resample all EEG signals to a certain frequency (such as 256hz) and then filter (for example, using filters to remove low-frequency, high-frequency and power noise, such as 0.1Hz

TABLE III: Datasets for pretraining and downstream tasks(continued1)

	Pretraining Datasets	Downstream Datasets
EEGPT1 [24]	PhysioMI [84]	BCIC-2A [77]
	HGD [85]	BCIC-2B [86]
	TSU [87]	Sleep-EDFx [49]
	SEED [70]	KaggleERN [61]
	M3CV [88]	PhysioP300 [84]
	-	TUAB [57]
	-	TUEV [57]
FoME [26]	TUEG [46]	TUEV [57]
	SEED [70]	SEED [70]
	SEED-IV [71]	SEED-IV [71]
	CHB-MIT [41]	CHB-MIT [41]
	Sleep-EDFx [49]	Sleep-EDFx [49]
	MI-Dataset [63]	MAYO [37]
	MAYO [37]	FNUSA [37]
	FNUSA [37]	-
EEGPT2 [27]	FACED [89]	FACED [89]
	SEED [70]	DEAP [90]
	SEED-FRA [91]	SEED-IV [71]
	SEED-GER [71]	SEED-V [60]
	SEED-IV [71]	MIBCI [92]
	SEED-V [60]	BCIC4-1 [56]
	THINGS-EEG-10Hz [93]	EEGMat [94]
	THINGS-EEG-5Hz [95]	EDF [49]
	IMG(*)	HMC [96]
	-	IMG(*)
	-	SPE [97]
	-	DREAMER [98]
MBrain [28]	SEEG(*)	SEEG(*)
	TUSZ [57]	TUSZ [57]

** Indicates the dataset may be private and the authors have not explicitly cited any literature in the paper.
* Indicates the corresponding dataset is private .
The data not cited any literature in the table are not mentioned in the corresponding article.

and 100Hz bandpass filters and 50Hz notch filters) and then standardize. This process helps to unify the data format and reduce data inconsistency, so that the model can learn features from it more effectively. We have counted the preprocessing of EEG signals for all models, see the Tab.V.

Most EEG-FMs perform minimal and simple data preprocessing steps, namely filtering and resampling, to standardize EEGs from various sources. Notably, the removal of noise-related outliers, suppression of EEG artifacts, artifactual EEG components, and site-related harmonization were not explicitly pursued. Moreover, data normalization strategies that produce training-ready samples were not sufficiently described in most studies. It remains unclear whether or how various offline data handling strategies impact EEG-FM pretraining and downstream task performance.

C. Parameter Size

In the pre-training of EEG-FM, the parameter size of the EEG-FM depends on multiple factors, including the model architecture, the number of layers, the number of neurons in each layer, and the dimension of the input data. In this section, we collect the parameter sizes of all large models, see the TabVI.

Aside from ALFEE [32], few EEG-FM related papers have examined and analyzed the impact of model and data scaling on task performance. Regarding model scaling, most papers

TABLE IV: Datasets for pretraining and downstream tasks(continued2)

	Pretraining Datasets	Downstream Datasets
BrainBERT [25]	-	-
NeuroLM [29]	TUEG [46]	-
	SEED [70]	TUAB [57]
	SEED-FRA [91]	TUEV [57]
	SEED-GER [71]	SEED [70]
	SEED-IV [71]	HMC [96]
	SEED-V [60]	EEGMat [94]
	BCIC4-1 [56]	TUSL [69]
	Emobrain [58]	-
	Grasp and Lift [59]	-
	MMI [63]	-
	RAW [64]	-
	RSEEG [65]	-
	Siena [43]	-
	SPIS [99]	-
	TVNT [66]	-
	**	-
CBraMod [30]	TUEG [46]	FACED [89]
	-	SEED-V [60]
	-	PhysioMI [84]
	-	SHU-MI [84]
	-	ISRUC [100]
	-	CHB-MIT [41]
	-	BCIC2020-3 [101]
	-	MDD-64 [45]
	-	SEED-VIG [102]
	-	EEGMat [94]
	-	TUEV [57]
	-	TUAB [57]
EEGFormer [31]	TUEG [46]	TUAB [57]
	-	TUAR [67]
	-	TUSL [69]
	-	TUSZ [57]
	-	Neonate [103]
ALFEE [32]	TUEG [46]	TUAB [57]
	SEED-IV [71]	TUAR [67]
	SEED-V [60]	TUSL [69]
	SEED-GER [71]	TUSZ [57]
	SEED-FRA [91]	Neonate [103]
	BCIC4-1 [56]	TUAB [57]
	Emobrain [58]	TUEV [57]
	Grasp and Lift [59]	SEED [70]
	Inria BCI [61]	HMC [96]
	MMI [63]	TUSL [69]
	RSEEG [65]	Workload [94]
	RawEEG [104]	-
	Siena [43]	-
	SPIS [99]	-
	TVNT [66]	-

** Indicates the dataset may be private and the authors have not explicitly cited any literature in the paper.
* Indicates the corresponding dataset is private .
The data not cited any literature in the table are not mentioned in the corresponding article.

lack comprehensive experimental evidence, making it unclear whether a clear trend in model scaling exists. Regarding data scaling, some papers conclude that increasing preprocessed data may lead to poorer performance on downstream tasks or the evidence for data scaling is weak. ALFEE [32] demonstrates that both model and data scaling apply equally to EEG-FM, with larger models and more preprocessed data generally resulting in better performance.

TABLE V: The preprocessing conditions of EEG datasets

Model	Resample	Filtering	Standardize
Brant [19]	✓, 250Hz	×	×
Brant-2 [20]	✓	✓	×
LaBraM [21]	✓, 200Hz	✓	✓
NeuroGPT [22]	✓, 250Hz	✓	✓
BIOT [23]	✓	×	✓
EEGPT1 [24]	✓, 256Hz	✓	✓
BrainBERT [25]	✓	✓	✓
FoME [26]	✓, 250Hz	✓	✓
EEGPT2 [27]	✓, 256Hz	✓	✓
MBrain [28]	×	×	×
NeuroLM [29]	✓, 200Hz	✓	✓
CBraMod [30]	✓, 200Hz	✓	✓
EEGFormer [31]	×	×	×
ALFEE [32]	✓, 256Hz	✓	✓

1. - Indicates that the corresponding article does not explicitly mention the size or length of EEG datasets for pre-training.
2. It is worth noting that Brant-2 [20] did not uniformly resample the pre-training data in the resampling, which allowed for brain recordings of varying lengths, sampling rates, and electrode counts, enhancing the flexibility of BrainWave for joint pretraining and deployment on iEEG and EEG data.
3. BIOT [23] conducted Ablation Study on Target Resampling Rate.
4. In Brant-2 [20], BIOT [23], BrainBERT [25] , the resampling frequency is different for different tasks.
5. MBrain [28] and EEGFormer [31] do not mention the description of data preprocessing.

TABLE VI: The parameter size of EEG-FMs.

Model	Model type	Size
Brant [19]	Brant	505.69M
Brant-2 [19]	Brant-2	-
LaBraM [21]	LaBraM-Base	5.8M
	LaBraM-Large	46M
	LaBraM-Huge	369M
NeuroGPT [22]	NeuroGPT	79.53M
BIOT [23]	BIOT	3.2M
EEGPT1 [24]	EEGPT-Tiny	4.7M
	EEGPT-Base	25M
BrainBERT [25]	BrainBERT	43.18M
FoME [26]	FoME-Base	476.3M
	FoME-Large	744.8M
EEGPT2 [25]	EEGPT-Base	1.46M
	EEGPT-Large	11.29M
	EEGPT-Huge	183.8M
	EEGPT-Giant	1.09B
MBrain [28]	MBrain	-
NeuroLM [29]	NeuroLM-B	254M
	NeuroLM-L	500M
	NeuroLM-XL	1696M
CBraMod [30]	CBraMod	4.0M
EEGFormer [31]	EEGFormer	-
ALFEE [32]	ALFEE-S	16.3M
	ALFEE-M	44.3M
	ALFEE-B	120M
	ALFEE-L	300M
	ALFEE-XL	540M

- Indicates that the corresponding article does not explicitly mention the parameter size of model.

D. Downstream Task Types

The performance of large EEG models is mainly evaluated through several types of downstream tasks, which can be divided into the following categories:

- Classification Tasks: These include emotion recognition, seizure detection, cognitive state classification, sleep stage identification, and motor imagery recognition.

- Short-term Prediction: These tasks involve predicting EEG signal trends or cognitive states over short time horizons.
- Long-term Prediction: Long-term prediction tasks focus on forecasting EEG signal patterns or brain state transitions over extended periods. These tasks are essential for applications such as neurodegenerative disease monitoring or long-term cognitive assessment.
- Imputation: EEG signal imputation addresses the challenge of missing or corrupted data segments.

At the same time, ablation experiments and model analysis are also essential. This section mainly summarizes the downstream tasks and model evaluation methods selected by these EEG-FMs, see TabVII.

E. Self-Supervise Learning

Self-supervised representation learning is a powerful approach to extract high level abstract representation from unlabelled data. Among those methods to learn representation via self-supervised pre-training, masked autoencoder (MAE) has been proved to be a simple but effective way in many fields [13], [16], [33]. After preprocessing all datasets involved in pre-training, we further organize the data into multiple signal blocks with approximately equal data volumes. The model treats each signal block as the minimal input unit. This enables cyclical pre-training on multiple datasets. We begin by segmenting the input signal into patches and randomly replacing a certain percentage(e.g. 40%) of the patches with learnable mask embeddings [MASK]. Then the generalization of the EEG-FM is enhanced by minimizing the reconstruction loss. It should be noted that the reconstruction objectives of different models are different, see the TabVIII.

F. Hardware for pretraining

In this section we summarize the hardware conditions for the pre-training of EEG-FM, see the Tab.IX.

IV. DISCUSSION

A. Current Research Challenges

Effects of Preprocessing and Normalization: EEG datasets may require extensive offline preprocessing to manage data quality and suppress artifacts. Because the current study performed minimal processing, it is unclear whether data outliers and noise impact EEG-FM preprocessing and task performance. Even clean EEG datasets require careful consideration of normalization strategies, as EEG can vary across channels, subjects, and acquisition sites [105]. Therefore, there is a need to better understand the impact of these choices on downstream EEG-FM modeling.

Standardized Benchmark Tasks: The lack of common tasks in EEG-FM evaluation makes understanding the state of the art challenging and highlights the need to identify a common core evaluation set for future EEG-FM evaluation. This set must cover a variety of task types, including classification and regression, and have both dense (one label for the entire EEG recording) and sparse (one label for each

TABLE VII: The types of downstream tasks

Model	Classification	Short-term Prediction	Long-term Prediction	Imputation	Others
Brant [19]	Seizure detection	✓	✓	✓	Frequency-phase forecasting
Brant-2 [20]	Alzheimer's disease diagnosis Seizure detection MDD diagnosis Depression diagnosis Schizophrenia diagnosis ADHD diagnosis Sleep deprivation detection	✗	✗	✗	-
LaBraM [21]	Abnormal detection Event type classification Emotion recognition	✗	✗	✗	Regression
NeuroGPT [22]	Motor Imagery classification	✗	✗	✗	-
BIOT [23]	Seizure detection Event type classification Seizure type classification Arrhythmias phenotype prediction Huamn action recognition	✗	✗	✗	-
EEGPT1 [24]	Abnormal detection Event type classification Motor Imagery classification Sleep stage detection Error related negativity detection Event-related potentials detection	✗	✗	✗	-
BrainBERT [25]	Sentence onset Speech vs. non-speech Volume Pitch	✗	✗	✗	-
FoME [26]	Seizure detection Sleep stage detection Emotion recognition Event type classification	✓	✓	✓	-
EEGPT2 [27]	Emotion Recognition Motor Imagery classification Mental workload detection Sleeping stage detection Cross Modality	✗	✗	✗	-
MBrain [28]	Seizure detection Emotion recognition	✗	✗	✗	-
NeuroLM [29]	Abnormal detection Event Type Classification Emotion Recognition Sleep Stage Classification Workload Detection Slowing Event Detection	✗	✗	✗	-
CBraMod [30]	Abnormal detection Event Type Classification Emotion Recognition Sleep Stage Classification Mental Stress Detection Vigilance Estimation Seizure Detection Imagined Speech Classification Motor Imagery Classification MDD Diagnosis	✗	✗	✗	-
EEGFormer [31]	Abnormal detection Event Type Classification Slowing Event Detection Seizure Detection	✗	✗	✗	-
ALFEE [32]	Abnormal detection Event Type Classification Emotion Recognition Sleep Stage Classification Workload Detection Slowing Event Detection	✗	✗	✗	-

1. MDD stands for Major Depressive Disorder.
2. ADHD stands for Attention deficit hyperactivity disorder.

TABLE VIII: The reconstruction objectives of EEG-FM

Model	Reconstruction Objective	Loss Function
Brant [19]	Original patches	$\mathcal{L}_{op}$
Brant-2 [20]	Embedded tokens	$\mathcal{L}_{pe}$
LaBraM [21]	Fourier Spectrum prediction Codebook prediction	$\mathcal{L}_A + \mathcal{L}_\phi + \mathcal{L}_{nnt} + \mathcal{L}_{eq}$
NeuroGPT [22]	Embedded tokens	$\mathcal{L}_{pe}$
BIOT [23]	Embedded tokens	$\mathcal{L}_{pe}$
EEGPT1 [24]	Original patches	$\mathcal{L}_{op}$
BrainBERT [25]	Masked spectrogram	$\mathcal{L}_{pe}$
FoME [26]	Original patches	$\mathcal{L}_{op}$
EEGPT2 [27]	Original patches	$\mathcal{L}_{op}$
MBrain [28]	-	-
NeuroLM [29]	Original patches Frequency magnitude Codebook prediction	$\mathcal{L}_{op} + \mathcal{L}_\phi + \mathcal{L}_{nnt} + \mathcal{L}_{eq}$
CBraMod [30]	Original patches	$\mathcal{L}_{op}$
EEGFormer [31]	Original patches Codebook prediction	$\mathcal{L}_{op} + \mathcal{L}_{nnt} + \mathcal{L}_{eq}$
ALFEE [32]	EEG signal forecasting Original patches Task classification	see [32]

1. - Indicates that the corresponding article does not explicitly mention the reconstruction details of EEG-FM.
2. In LaBraM [21], the loss fails to converge while directly reconstructing raw EEG signals(Original patches).
3. NeuroLM [29] observes that reconstructing the phase contributes minor to neural tokenizer training.

TABLE IX: The hardware conditions for the pre-training of EEG-FM

Model	GPU	Time	Quantity
Brant [19]	NVIDIA Tesla A100	2.8 days	4
Brant-2 [20]	NVIDIA Tesla A100	100 hours	4
LaBraM [21]	NVIDIA A800	-	-
NeuroGPT [22]	-	-	-
BIOT [23]	NVIDIA RTX A6000	-	8
EEGPT1 [24]	NVIDIA RTX 3090	-	8
BrainBERT [25]	-	-	-
FoME [26]	NVIDIA RTX 4090	350 hours	6
EEGPT2 [27]	NVIDIA A800-SXM4	20 hours	8
MBrain [28]	-	-	-
NeuroLM [29]	NVIDIA Tesla A100	-	8
CBraMod [30]	NVIDIA RTX A5000	5 days	4
EEGFormer [31]	-	-	-
ALFEE [32]	NVIDIA A800	-	8

- Indicates that the corresponding article does not explicitly mention the hardware conditions for pre-training.

EEG segment) labels. Furthermore, some existing datasets may have saturated the performance of traditional methods [106], preventing them from fully exploring the potential of EEG-FM. Therefore, collecting and open-sourcing challenging new datasets is crucial for the future development of EEG-FM.

Long-Term Context Modeling: The required EEG recording duration depends on the signal-to-noise ratio of the target neural signal, the statistical requirements for improving the signal-to-noise ratio through repeated sampling, and the temporal characteristics of the brain activity being studied.These include:

- Transient events (milliseconds to seconds): ERPs [107]–[110], such as the P300 (peak approximately 300 ms after stimulus), the N170 (peak approximately 170 ms), and the error-related negativity (ERN, peak approximately 100 ms after the response), are brief, rapid responses to discrete stimuli or events. The "unit of analysis" here is a short time window (epoch) surrounding the event, typically 1-2 seconds.
- Rhythmic states (seconds to minutes): Resting-state or task-state [111] EEG analysis focuses on persistent EEG oscillations that remain relatively stable over several minutes, such as alpha, beta and specific task-related rhythms. In these cases, the "unit of analysis" is a continuous recording lasting several minutes.
- Evolutionary states (tens of minutes to hours): Cognitive states [112]–[115], such as driving fatigue and mental workload, evolve gradually during task performance. The "unit of analysis" here is the duration of the entire task, as the study is precisely about changes in states over time.
- Macrostructural Patterns (Hours): Sleep staging [116], [117] aims to observe the complete structure of sleep, including multiple approximately 90-minute cycles of non-rapid eye movement (NREM) and rapid eye movement (REM) sleep. This requires a full night of recording, typically 6-8 hours. The "unit of analysis" is the entire sleep period.

Trustworthy Modeling: Currently, no EEG-FMs focus on model interpretability or explanation, which remains a key requirement for data-driven modeling in high-stakes and expert-centric medical fields. Research is needed to uncover the black box of EEG-FMs and gain insights into the actual robustness of their decision-making processes, both in pre-training and in downstream applications. Linking to known brain physiological or pathological patterns may be necessary for expert users to better assist in EEG-based diagnosis of disorders (such as ASD, ADHD, and MDD).

B. Performance Evaluation

One of the most significant obstacles in current EEG-FM research is the lack of standardized evaluation protocols and benchmarks [118]. Different studies evaluate their models on a wide range of downstream tasks and datasets, making direct and fair comparisons nearly impossible. For example, one model may perform well on a seizure detection task, while another performs poorly on an emotion recognition task. Even for the same task (e.g., motor imagery), the datasets, preprocessing pipelines, and data partitioning strategies (e.g., within-subject vs. between-subject cross-validation) used can vary, making performance results incomparable. This heterogeneity hinders a clear understanding of true progress in the field. To address this issue, the research community urgently needs to develop and adopt standardized benchmark suites, such as emerging initiatives like AdaBrain-Bench [119][11], which aims to provide a framework covering a variety of BCI tasks, multi-dimensional evaluation metrics, and standardized adaptation procedures. Such benchmarks will provide a level playing field for evaluating generalization across subjects, tasks, and datasets.

Many models are evaluated under flawed settings. A common problem is "in-sample" evaluation, where the downstream

[11] https://github.com/Jamine-W/AdaBrain-Bench

task data used for fine-tuning and testing is itself part of the pre-training dataset. This approach fails to truly test the model's generalization ability to new, unseen data. A more rigorous and realistic evaluation metric is "out-of-distribution" (OOD) evaluation, where model performance is tested on datasets completely unseen during model pre-training. This simulates real-world scenarios when deploying the model to a new hospital or using it with new hardware. Furthermore, the evaluation should clearly distinguish between cross-subject generalization (i.e., performance on new subjects in the same dataset) and the more challenging cross-dataset generalization (i.e., performance on datasets from different studies with different protocols and hardware). Only through rigorous OOD and cross-dataset testing can we truly trust that the model has learned universal neurophysiological representations, rather than biases or artifacts from a specific dataset.

In addition, methods for evaluating EEG-FM capabilities also need to diversify. Currently, the dominant evaluation paradigm is to fully fine-tune the entire pre-trained model on a downstream task. While this demonstrates the model's best potential performance, it does not fully reveal the intrinsic quality of the representations learned during pre-training [120].

- Linear probing: In this strategy, the pre-trained encoder weights are frozen, and only a simple linear classifier is trained on top of them. The performance of linear probing directly reflects the quality and separability of the learned representations. However, many studies have reported that linear probing performs significantly worse than full fine-tuning, raising questions about the intrinsic quality of representations learned by current self-supervised learning strategies.
- Few-Shot and Zero-Shot Learning: This is a critical test of the capabilities of a base model. Evaluating a model's ability to handle new tasks with only minimal (few-shot) or even no (zero-shot) labeled training examples is central to measuring its true utility as a general-purpose feature extractor.

Finally, evaluation metrics themselves need to go beyond traditional classification accuracy to better reflect the model's actual clinical or application value. For example, in epilepsy detection tasks, false positives per hour is a more clinically relevant metric than the F1 score because it directly relates to alarm fatigue and clinical workflow [121]. Similarly, when assessing continuous states such as stress or fatigue, models must not only be accurate but also capable of early prediction [122], which requires specialized evaluation metrics. Therefore, future evaluation frameworks should integrate more application-specific and meaningful metrics to comprehensively assess a model's real-world utility.

C. Future Directions

Although great progress has been made in the research of EEG foundation models, several promising directions can still be found in the rapidly developing field of EEG-FM research.

First, almost all current EEG-FMs use a self-supervised learning framework with masks. The key operation to achieve this is to segment the EEG signal into blocks, inspired by block embeddings in images. A comprehensive comparison of the various detailed parameters of EEG segmentation (e.g. the architecture settings of EEG-FM, the sampling rate of the EEG signal, the length of the EEG patches, the overlap rate between the EEG patches, the percentage of data masked in self-supervised training and the selection of pre-training datasets) with respect to their influence on downstream tasks performance should be carried out to address this crucial design question in a systematic manner. Only articles [22], [23] reported the impact of various detailed parameters of EEG segmentation on the experimental results: Article [22] mentioned that increasing the length of patches, increasing the number of patches, reducing the overlapping ratio, increasing the embedding dimension, and increasing the number of self-attention layers in the encoder can enhance the model performance of downstream tasks, the article does not provide convincing data and charts to prove its conclusions. Article [23] mentioned that increasing the length of blocks, the sampling rate of the EEG signal and increasing the overlapping ratio can enhance the model performance of downstream tasks with detailed ablation experiments. However, their views differ in the overlapping ratio.

Secondly, GNN can be considered to capture the spatial pattern of EEG signals. We found that EEGPT2 [27] and [123] has tried to integrate GNN into EEG-FM to better capture the potential spatial features of EEG signals. Thirdly, the number of parameters of EEG-FM is still small compared to the current mainstream large language models(e.g. ChatGPT-4o). How to design models that fit specific tasks well but have small parameters, and how to design models with large parameters and strong generalization will be the focus of future work. Fourthly, designing a model that generates EEG signals from language will be a competitive direction, which may solve the problem of lack of model pre-training EEG signals. Finally, current work primarily focuses on robust EEG representation, further research is needed to extend the model to multimodal scenarios such as Video-EEG, Image-EEG, and Text-EEG. Therefore, combining EEG models with other modes such as language and imaging to create multimodal vertical fields EEG-FM is expected to create an overall framework connecting neuroscience and artificial intelligence, opening up new avenues for research and application.

V. CONCLUSION

EEG-FMs have become a powerful tool for analyzing and understanding EEG signals. Through their advanced architectures and pre-training strategies, these models have achieved superior performance in various tasks, including disease diagnosis, sleep monitoring, and emotion classification. In this article, we summarize various details of EEG-FMs, including pre-training techniques, pre-training datasets, downstream task datasets, etc. As EEG-based models continue to advance, their transformative impact on healthcare, neuroscience, and brain-computer interface technology is expected to grow, bridging the gap between theoretical progress and practical applications.

In summary, EEG-FMs are expected to improve our understanding of the brain and develop new applications in neuroscience and healthcare. Continued research and innovation

in this field will help develop more accurate, efficient, and interpretable EEG-FM, ultimately achieving better diagnosis, treatment, and rehabilitation of neurological diseases.

REFERENCES

[1] Xiang Li, Yazhou Zhang, Prayag Tiwari, Dawei Song, Bin Hu, Meihong Yang, Zhigang Zhao, Neeraj Kumar, and Pekka Marttinen. Eeg based emotion recognition: A tutorial and review. *ACM Computing Surveys*, 55(4):1–57, 2022.

[2] Eunjin Jeon, Wonjun Ko, Jee Seok Yoon, and Heung-Il Suk. Mutual information-driven subject-invariant and class-relevant deep representation learning in bci. *IEEE Transactions on Neural Networks and Learning Systems*, 34(2):739–749, 2021.

[3] Yang Du, Yongling Xu, Xiaoan Wang, Li Liu, and Pengcheng Ma. Eeg temporal–spatial transformer for person identification. *Scientific Reports*, 12(1):14378, 2022.

[4] Poomipat Boonyakitanont, Apiwat Lek-Uthai, Krisnachai Chomtho, and Jitkomut Songsiri. A review of feature extraction and performance evaluation in epileptic seizure detection using eeg. *Biomedical Signal Processing and Control*, 57:101702, 2020.

[5] Lakhan Dev Sharma, Vijay Kumar Bohat, Maria Habib, Al-Zoubi Ala'M, Hossam Faris, and Ibrahim Aljarah. Evolutionary inspired approach for mental stress detection using eeg signal. *Expert systems with applications*, 197:116634, 2022.

[6] Khald Ali I Aboalayon, Miad Faezipour, Wafaa S Almuhammadi, and Saeid Moslehpour. Sleep stage classification using eeg signal analysis: a comprehensive survey and new investigation. *Entropy*, 18(9):272, 2016.

[7] Syed Umar Amin, Mansour Alsulaiman, Ghulam Muhammad, Mohamed Amine Mekhtiche, and M Shamim Hossain. Deep learning for eeg motor imagery classification based on multi-layer cnns feature fusion. *Future Generation computer systems*, 101:542–554, 2019.

[8] Subhrajit Roy, Isabell Kiral-Kornek, and Stefan Harrer. Chrononet: A deep recurrent neural network for abnormal eeg identification. In *Artificial Intelligence in Medicine: 17th Conference on Artificial Intelligence in Medicine, AIME 2019, Poznan, Poland, June 26–29, 2019, Proceedings 17*, pages 47–56. Springer, 2019.

[9] Nazmi Sofian Suhaimi, James Mountstephens, and Jason Teo. Eeg-based emotion recognition: a state-of-the-art review of current trends and opportunities. *Computational intelligence and neuroscience*, 2020(1):8875426, 2020.

[10] Wouter Biesmans, Neetha Das, Tom Francart, and Alexander Bertrand. Auditory-inspired speech envelope extraction methods for improved eeg-based auditory attention detection in a cocktail party scenario. *IEEE transactions on neural systems and rehabilitation engineering*, 25(5):402–412, 2016.

[11] Yudhajit Das, Hanli Liu, Fenghua Tian, Srinivas Kota, Rong Zhang, and Lina F Chalak. Rigor of neurovascular coupling (nvc) assessment in newborns using different amplitude eeg algorithms. *Scientific reports*, 10(1):9183, 2020.

[12] Yiping Wang, Yanfeng Yang, Gongpeng Cao, Jinjie Guo, Penghu Wei, Tao Feng, Yang Dai, Jinguo Huang, Guixia Kang, and Guoguang Zhao. Seeg-net: An explainable and deep learning-based cross-subject pathological activity detection method for drug-resistant epilepsy. *Computers in Biology and Medicine*, 148:105703, 2022.

[13] Jacob Devlin. Bert: Pre-training of deep bidirectional transformers for language understanding. *arXiv preprint arXiv:1810.04805*, 2018.

[14] Libo Qin, Qiguang Chen, Xiachong Feng, Yang Wu, Yongheng Zhang, Yinghui Li, Min Li, Wanxiang Che, and Philip S Yu. Large language models meet nlp: A survey. *arXiv preprint arXiv:2405.12819*, 2024.

[15] Xinlei Chen, Saining Xie, and Kaiming He. An empirical study of training self-supervised vision transformers. In *Proceedings of the IEEE/CVF international conference on computer vision*, pages 9640–9649, 2021.

[16] Kaiming He, Xinlei Chen, Saining Xie, Yanghao Li, Piotr Dollár, and Ross Girshick. Masked autoencoders are scalable vision learners. In *Proceedings of the IEEE/CVF conference on computer vision and pattern recognition*, pages 16000–16009, 2022.

[17] Raby Hamadi. Large language models meet computer vision: A brief survey. *arXiv preprint arXiv:2311.16673*, 2023.

[18] Jonathan W Kim, Ahmed Alaa, and Danilo Bernardo. Eeg-gpt: exploring capabilities of large language models for eeg classification and interpretation. *arXiv preprint arXiv:2401.18006*, 2024.

[19] Daoze Zhang, Zhizhang Yuan, Yang Yang, Junru Chen, Jingjing Wang, and Yafeng Li. Brant: Foundation model for intracranial neural signal. *Advances in Neural Information Processing Systems*, 36, 2024.

[20] Zhizhang Yuan, Daoze Zhang, Junru Chen, Geifei Gu, and Yang Yang. Brant-2: Foundation model for brain signals. *arXiv preprint arXiv:2402.10251*, 2024.

[21] Wei-Bang Jiang, Li-Ming Zhao, and Bao-Liang Lu. Large brain model for learning generic representations with tremendous eeg data in bci. *arXiv preprint arXiv:2405.18765*, 2024.

[22] Wenhui Cui, Woojae Jeong, Philipp Thölke, Takfarinas Medani, Karim Jerbi, Anand A Joshi, and Richard M Leahy. Neuro-gpt: Towards a foundation model for eeg. In *2024 IEEE International Symposium on Biomedical Imaging (ISBI)*, pages 1–5. IEEE, 2024.

[23] C Yang, MB Westover, and J Sun. Biot: Cross-data biosignal learning in the wild [internet]. arxiv; 2023 [cited 2023 may 30].

[24] Guangyu Wang, Wenchao Liu, Yuhong He, Cong Xu, Lin Ma, and Haifeng Li. Eegpt: Pretrained transformer for universal and reliable representation of eeg signals. In *The Thirty-eighth Annual Conference on Neural Information Processing Systems*, 2024.

[25] Christopher Wang, Vighnesh Subramaniam, Adam Uri Yaari, Gabriel Kreiman, Boris Katz, Ignacio Cases, and Andrei Barbu. Brainbert: Self-supervised representation learning for intracranial recordings. *arXiv preprint arXiv:2302.14367*, 2023.

[26] Enze Shi, Kui Zhao, Qilong Yuan, Jiaqi Wang, Huawen Hu, Sigang Yu, and Shu Zhang. Fome: A foundation model for eeg using adaptive temporal-lateral attention scaling. *arXiv preprint arXiv:2409.12454*, 2024.

[27] Tongtian Yue, Shuning Xue, Xuange Gao, Yepeng Tang, Longteng Guo, Jie Jiang, and Jing Liu. Eegpt: Unleashing the potential of eeg generalist foundation model by autoregressive pre-training. *arXiv preprint arXiv:2410.19779*, 2024.

[28] Donghong Cai, Junru Chen, Yang Yang, Teng Liu, and Yafeng Li. Mbrain: A multi-channel self-supervised learning framework for brain signals. In *Proceedings of the 29th ACM SIGKDD Conference on Knowledge Discovery and Data Mining*, pages 130–141, 2023.

[29] Wei-Bang Jiang, Yansen Wang, Bao-Liang Lu, and Dongsheng Li. Neurolm: A universal multi-task foundation model for bridging the gap between language and eeg signals. *arXiv preprint arXiv:2409.00101*, 2024.

[30] Jiquan Wang, Sha Zhao, Zhiling Luo, Yangxuan Zhou, Haiteng Jiang, Shijian Li, Tao Li, and Gang Pan. Cbramod: A criss-cross brain foundation model for eeg decoding. *arXiv preprint arXiv:2412.07236*, 2024.

[31] Yuqi Chen, Kan Ren, Kaitao Song, Yansen Wang, Yifan Wang, Dongsheng Li, and Lili Qiu. Eegformer: Towards transferable and interpretable large-scale eeg foundation model. *arXiv preprint arXiv:2401.10278*, 2024.

[32] Wei Xiong, Junming Lin, Jiangtong Li, Jie Li, and Changjun Jiang. Alfee: Adaptive large foundation model for eeg representation. *arXiv preprint arXiv:2505.06291*, 2025.

[33] Yuqi Nie, Nam H Nguyen, Phanwadee Sinthong, and Jayant Kalagnanam. A time series is worth 64 words: Long-term forecasting with transformers. *arXiv preprint arXiv:2211.14730*, 2022.

[34] HJ Landau. Sampling, data transmission, and the nyquist rate. *Proceedings of the IEEE*, 55(10):1701–1706, 1967.

[35] Ronald N Bracewell. The fourier transform. *Scientific American*, 260(6):86–95, 1989.

[36] Zhiliang Peng, Li Dong, Hangbo Bao, Qixiang Ye, and Furu Wei. Beit v2: Masked image modeling with vector-quantized visual tokenizers. *arXiv preprint arXiv:2208.06366*, 2022.

[37] Petr Nejedly, Vaclav Kremen, Vladimir Sladky, Jan Cimbalnik, Petr Klimes, Filip Plesinger, Filip Mivalt, Vojtech Travnicek, Ivo Viscor, Martin Pail, et al. Multicenter intracranial eeg dataset for classification of graphoelements and artifactual signals. *Scientific data*, 7(1):179, 2020.

[38] Dorien van Blooijs, Max A van den Boom, Jaap F van der Aar, Geertjan M Huiskamp, Giulio Castegnaro, Matteo Demuru, Willemiek JEM Zweiphenning, Pieter van Eijsden, Kai J Miller, Frans SS Leijten, et al. Developmental trajectory of transmission speed in the human brain. *Nature Neuroscience*, 26(4):537–541, 2023.

[39] Andreas Miltiadous, Katerina D Tzimourta, Theodora Afrantou, Panagiotis Ioannidis, Nikolaos Grigoriadis, Dimitrios G Tsalikakis, Pantelis Angelidis, Markos G Tsipouras, Evripidis Glavas, Nikolaos Giannakeas, et al. A dataset of eeg recordings from: Alzheimer's disease, frontotemporal dementia and healthy subjects. *OpenNeuro*, 1:88, 2023.

[40] Mario Giovanni Terzano, Liborio Parrino, Arianna Smerieri, Ronald Chervin, Sudhansu Chokroverty, Christian Guilleminault, Max Hirshkowitz, Mark Mahowald, Harvey Moldofsky, Agostino Rosa, et al. Atlas, rules, and recording techniques for the scoring of cyclic alternating pattern (cap) in human sleep. *Sleep medicine*, 3(2):187–199, 2002.

[41] J. Guttag. Chb-mit scalp eeg database (version 1.0.0). https://doi.org/10.13026/C2K01R, 2010. PhysioNet.

[42] Diego Alvarez-Estevez and Roselyne M Rijsman. Inter-database validation of a deep learning approach for automatic sleep scoring. *PloS one*, 16(8):e0256111, 2021.

[43] Paolo Detti, Giampaolo Vatti, and Garazi Zabalo Manrique de Lara. Eeg synchronization analysis for seizure prediction: A study on data of noninvasive recordings. *Processes*, 8(7):846, 2020.

[44] Christoffer Hatlestad-Hall, Trine Waage Rygvold, and Stein Andersson. Bids-structured resting-state electroencephalography (eeg) data extracted from an experimental paradigm. *Data in Brief*, 45:108647, 2022.

[45] Wajid Mumtaz. Mdd patients and healthy controls eeg data (new). *Figshare, Dataset*, 2016.

[46] Amir Harati, Silvia Lopez, I Obeid, J Picone, MP Jacobson, and S Tobochnik. The tuh eeg corpus: A big data resource for automated eeg interpretation. In *2014 IEEE signal processing in medicine and biology symposium (SPMB)*, pages 1–5. IEEE, 2014.

[47] OpenNeuro. ds003478: [dataset title]. https://openneuro.org/datasets/ds003478/versions/1.1.0, 2021. Version 1.1.0.

[48] Elzbieta Olejarczyk and Wojciech Jernajczyk. EEG in schizophrenia, 2017.

[49] Bob Kemp, Aeilko H Zwinderman, Bert Tuk, Hilbert AC Kamphuisen, and Josefien JL Oberye. Analysis of a sleep-dependent neuronal feedback loop: the slow-wave microcontinuity of the eeg. *IEEE Transactions on Biomedical Engineering*, 47(9):1185–1194, 2000.

[50] Ghasem Sadeghi Bajestani, Shima Abedian, Fatemeh Makhloughi, Motahhareh Raoufitabar, and Hamid Saeedi. A dataset of eeg signals from adults with adhd and healthy controls: Resting state, cognitive function, and sound listening paradigm. https://doi.org/10.17632/6k4g25fhzg.1, 2023. Mendeley Data, V1.

[51] Haijie Liu and Xiaodong Lv. EEG datasets of stroke patients. 12 2022.

[52] Ali Motie Nasrabadi, Armin Allahverdy, Mehdi Samavati, and Mohammad Reza Mohammadi. Eeg data for adhd / control children, 2020.

[53] AP Rockhill, N Jackson, JS George, AR Aron, and NC Swann. Uc san diego resting state eeg data from patients with parkinson's disease. openneuro [dataset], 2021.

[54] Chuqin Xiang, Xinrui Fan, Duo Bai, Ke Lv, and Xu Lei. A resting-state eeg dataset for sleep deprivation. *Scientific Data*, 11(1):427, 2024.

[55] Mário L Vicchietti, Fernando M Ramos, Luiz E Betting, and Andriana SLO Campanharo. Computational methods of eeg signals analysis for alzheimer's disease classification. *Scientific Reports*, 13(1):8184, 2023.

[56] Benjamin Blankertz, Guido Dornhege, Matthias Krauledat, Klaus-Robert Müller, and Gabriel Curio. The non-invasive berlin brain–computer interface: fast acquisition of effective performance in untrained subjects. *NeuroImage*, 37(2):539–550, 2007.

[57] Iyad Obeid and Joseph Picone. The temple university hospital eeg data corpus. *Frontiers in neuroscience*, 10:196, 2016.

[58] Arman Savran, Koray Ciftci, Guillame Chanel, Javier Cruz_Mota, Luong Hong Viet, Bülent Sankur, Lale Akarun, Alice Caplier, and Michele Rombaut. Emotion detection in the loop from brain signals and facial images. In *eINTERFACE'06-SIMILAR NoE Summer Workshop on Multimodal Interfaces*, 2006.

[59] Matthew D Luciw, Ewa Jarocka, and Benoni B Edin. Multi-channel eeg recordings during 3,936 grasp and lift trials with varying weight and friction. *Scientific data*, 1(1):1–11, 2014.

[60] Wei Liu, Jie-Lin Qiu, Wei-Long Zheng, and Bao-Liang Lu. Comparing recognition performance and robustness of multimodal deep learning models for multimodal emotion recognition. *IEEE Transactions on Cognitive and Developmental Systems*, 14(2):715–729, 2021.

[61] Perrin Margaux, Maby Emmanuel, Daligault Sébastien, Bertrand Olivier, and Mattout Jérémie. Objective and subjective evaluation of online error correction during p300-based spelling. *Advances in Human-Computer Interaction*, 2012(1):578295, 2012.

[62] Yongtian He, Trieu Phat Luu, Kevin Nathan, Sho Nakagome, and Jose L Contreras-Vidal. A mobile brain-body imaging dataset recorded during treadmill walking with a brain-computer interface. *Scientific data*, 5(1):1–10, 2018.

[63] Gerwin Schalk, Dennis J McFarland, Thilo Hinterberger, Niels Birbaumer, and Jonathan R Wolpaw. Bci2000: a general-purpose brain-computer interface (bci) system. *IEEE Transactions on biomedical engineering*, 51(6):1034–1043, 2004.

[64] Texas Data Repository. Dataset title. https://dataverse.tdl.org/dataset.xhtml?persistentId=doi:10.18738/T8/SS2NHB, 2020. Accessed via Texas Data Repository.

[65] Logan T Trujillo, Candice T Stanfield, and Ruben D Vela. The effect of electroencephalogram (eeg) reference choice on information-theoretic measures of the complexity and integration of eeg signals. *Frontiers in neuroscience*, 11:425, 2017.

[66] Louis Korczowski, Martine Cederhout, Anton Andreev, Grégoire Cattan, Pedro Luiz Coelho Rodrigues, Violette Gautheret, and Marco Congedo. *Brain Invaders calibration-less P300-based BCI with modulation of flash duration Dataset (bi2015a)*. PhD thesis, GIPSA-lab, 2019.

[67] G Buckwalter, S Chhin, S Rahman, I Obeid, and J Picone. Recent advances in the tuh eeg corpus: improving the interrater agreement for artifacts and epileptiform events. In *2021 IEEE Signal Processing in Medicine and Biology Symposium (SPMB)*, pages 1–3. IEEE, 2021.

[68] L Veloso, J McHugh, E Von Weltin, S Lopez, I Obeid, and J Picone. Big data resources for eegs: Enabling deep learning research. In *2017 IEEE Signal Processing in Medicine and Biology Symposium (SPMB)*, pages 1–3. IEEE, 2017.

[69] Eva von Weltin, Tameem Ahsan, Vinit Shah, Dawer Jamshed, Meysam Golmohammadi, Iyad Obeid, and Joseph Picone. Electroencephalographic slowing: A primary source of error in automatic seizure detection. In *2017 IEEE Signal Processing in Medicine and Biology Symposium (SPMB)*, pages 1–5. IEEE, 2017.

[70] Wei-Long Zheng and Bao-Liang Lu. Investigating critical frequency bands and channels for eeg-based emotion recognition with deep neural networks. *IEEE Transactions on autonomous mental development*, 7(3):162–175, 2015.

[71] Wei-Long Zheng, Wei Liu, Yifei Lu, Bao-Liang Lu, and Andrzej Cichocki. Emotionmeter: A multimodal framework for recognizing human emotions. *IEEE transactions on cybernetics*, 49(3):1110–1122, 2018.

[72] Wei-Bang Jiang, Xuan-Hao Liu, Wei-Long Zheng, and Bao-Liang Lu. Multimodal adaptive emotion transformer with flexible modality inputs on a novel dataset with continuous labels. In *Proceedings of the 31st ACM International Conference on Multimedia*, pages 5975–5984, 2023.

[73] Wei-Bang Jiang, Li-Ming Zhao, Ping Guo, and Bao-Liang Lu. Discriminating surprise and anger from eeg and eye movements with a graph network. In *2021 IEEE International Conference on Bioinformatics and Biomedicine (BIBM)*, pages 1353–1357. IEEE, 2021.

[74] Shuai Luo, Yu-Ting Lan, Dan Peng, Ziyi Li, Wei-Long Zheng, and Bao-Liang Lu. Multimodal emotion recognition in response to oil paintings. In *2022 44th Annual International Conference of the IEEE Engineering in Medicine & Biology Society (EMBC)*, pages 4167–4170. IEEE, 2022.

[75] Rui Li, Le-Dian Liu, and Bao-Liang Lu. Discrimination of decision confidence levels from eeg signals. In *2021 10th International IEEE/EMBS Conference on Neural Engineering (NER)*, pages 946–949. IEEE, 2021.

[76] Le-Yan Tao and Bao-Liang Lu. Emotion recognition under sleep deprivation using a multimodal residual lstm network. In *2020 International Joint Conference on Neural Networks (IJCNN)*, pages 1–8. IEEE, 2020.

[77] Michael Tangermann, Klaus-Robert Müller, Ad Aertsen, Niels Birbaumer, Christoph Braun, Clemens Brunner, Robert Leeb, Carsten Mehring, Kai J Miller, Gernot R Müller-Putz, et al. Review of the bci competition iv. *Frontiers in neuroscience*, 6:55, 2012.

[78] Guo-Qiang Zhang, Licong Cui, Remo Mueller, Shiqiang Tao, Matthew Kim, Michael Rueschman, Sara Mariani, Daniel Mobley, and Susan Redline. The national sleep research resource: towards a sleep data commons. *Journal of the American Medical Informatics Association*, 25(10):1351–1358, 2018.

[79] Stuart F Quan, Barbara V Howard, Conrad Iber, James P Kiley, F Javier Nieto, George T O'Connor, David M Rapoport, Susan Redline, John Robbins, Jonathan M Samet, et al. The sleep heart health study: design, rationale, and methods. *Sleep*, 20(12):1077–1085, 1997.

[80] Erick A Perez Alday, Annie Gu, Amit J Shah, Chad Robichaux, An-Kwok Ian Wong, Chengyu Liu, Feifei Liu, Ali Bahrami Rad, Andoni Elola, Salman Seyedi, et al. Classification of 12-lead ecgs: the physionet/computing in cardiology challenge 2020. *Physiological measurement*, 41(12):124003, 2020.

[81] Wendong Ge, Jin Jing, Sungtae An, Aline Herlopian, Marcus Ng, Aaron F Struck, Brian Appavu, Emily L Johnson, Gamaleldin Osman,

Hiba A Haider, et al. Deep active learning for interictal ictal injury continuum eeg patterns. *Journal of neuroscience methods*, 351:108966, 2021.

[82] Patrick Wagner, Nils Strodthoff, Ralf-Dieter Bousseljot, Dieter Kreiseler, Fatima I Lunze, Wojciech Samek, and Tobias Schaeffter. Ptb-xl, a large publicly available electrocardiography dataset. *Scientific data*, 7(1):1–15, 2020.

[83] Davide Anguita, Alessandro Ghio, Luca Oneto, Xavier Parra, Jorge Luis Reyes-Ortiz, et al. A public domain dataset for human activity recognition using smartphones. In *Esann*, volume 3, page 3, 2013.

[84] Ary L Goldberger, Luis AN Amaral, Leon Glass, Jeffrey M Hausdorff, Plamen Ch Ivanov, Roger G Mark, Joseph E Mietus, George B Moody, Chung-Kang Peng, and H Eugene Stanley. Physiobank, physiotoolkit, and physionet: components of a new research resource for complex physiologic signals. *circulation*, 101(23):e215–e220, 2000.

[85] Robin Tibor Schirrmeister, Jost Tobias Springenberg, Lukas Dominique Josef Fiederer, Martin Glasstetter, Katharina Eggensperger, Michael Tangermann, Frank Hutter, Wolfram Burgard, and Tonio Ball. Deep learning with convolutional neural networks for eeg decoding and visualization. *Human brain mapping*, 38(11):5391–5420, 2017.

[86] David Steyrl, Reinhold Scherer, Josef Faller, and Gernot R Müller-Putz. Random forests in non-invasive sensorimotor rhythm brain-computer interfaces: a practical and convenient non-linear classifier. *Biomedical Engineering/Biomedizinische Technik*, 61(1):77–86, 2016.

[87] Yijun Wang, Xiaogang Chen, Xiaorong Gao, and Shangkai Gao. A benchmark dataset for ssvep-based brain–computer interfaces. *IEEE Transactions on Neural Systems and Rehabilitation Engineering*, 25(10):1746–1752, 2016.

[88] Gan Huang, Zhenxing Hu, Weize Chen, Shaorong Zhang, Zhen Liang, Linling Li, Li Zhang, and Zhiguo Zhang. M3cv: A multi-subject, multi-session, and multi-task database for eeg-based biometrics challenge. *NeuroImage*, 264:119666, 2022.

[89] Jingjing Chen, Xiaobin Wang, Chen Huang, Xin Hu, Xinke Shen, and Dan Zhang. A large finer-grained affective computing eeg dataset. *Scientific Data*, 10(1):740, 2023.

[90] Sander Koelstra, Christian Muhl, Mohammad Soleymani, Jong-Seok Lee, Ashkan Yazdani, Touradj Ebrahimi, Thierry Pun, Anton Nijholt, and Ioannis Patras. Deap: A database for emotion analysis; using physiological signals. *IEEE transactions on affective computing*, 3(1):18–31, 2011.

[91] Wei Liu, Wei-Long Zheng, Ziyi Li, Si-Yuan Wu, Lu Gan, and Bao-Liang Lu. Identifying similarities and differences in emotion recognition with eeg and eye movements among chinese, german, and french people. *Journal of Neural Engineering*, 19(2):026012, 2022.

[92] Hohyun Cho, Minkyu Ahn, Sangtae Ahn, Moonyoung Kwon, and Sung Chan Jun. Eeg datasets for motor imagery brain–computer interface. *GigaScience*, 6(7):gix034, 2017.

[93] Tijl Grootswagers, Ivy Zhou, Amanda K Robinson, Martin N Hebart, and Thomas A Carlson. Human eeg recordings for 1,854 concepts presented in rapid serial visual presentation streams. *Scientific Data*, 9(1):3, 2022.

[94] Igor Zyma, Sergii Tukaev, Ivan Seleznov, Ken Kiyono, Anton Popov, Mariia Chernykh, and Oleksii Shpenkov. Electroencephalograms during mental arithmetic task performance. *Data*, 4(1):14, 2019.

[95] Alessandro T Gifford, Kshitij Dwivedi, Gemma Roig, and Radoslaw M Cichy. A large and rich eeg dataset for modeling human visual object recognition. *NeuroImage*, 264:119754, 2022.

[96] Diego Alvarez-Estevez and RM Rijsman. Haaglanden medisch centrum sleep staging database (version 1.0. 1). *PhysioNet*, 2021.

[97] Chuong H Nguyen, George K Karavas, and Panagiotis Artemiadis. Inferring imagined speech using eeg signals: a new approach using riemannian manifold features. *Journal of neural engineering*, 15(1):016002, 2017.

[98] Stamos Katsigiannis and Naeem Ramzan. Dreamer: A database for emotion recognition through eeg and ecg signals from wireless low-cost off-the-shelf devices. *IEEE journal of biomedical and health informatics*, 22(1):98–107, 2017.

[99] Mastaneh Torkamani-Azar, Sumeyra Demir Kanik, Serap Aydin, and Mujdat Cetin. Prediction of reaction time and vigilance variability from spatio-spectral features of resting-state eeg in a long sustained attention task. *IEEE journal of biomedical and health informatics*, 24(9):2550–2558, 2020.

[100] Sirvan Khalighi, Teresa Sousa, José Moutinho Santos, and Urbano Nunes. Isruc-sleep: A comprehensive public dataset for sleep researchers. *Computer methods and programs in biomedicine*, 124:180–192, 2016.

[101] Ji-Hoon Jeong, Jeong-Hyun Cho, Young-Eun Lee, Seo-Hyun Lee, Gi-Hwan Shin, Young-Seok Kweon, José del R Millán, Klaus-Robert Müller, and Seong-Whan Lee. 2020 international brain–computer interface competition: A review. *Frontiers in Human Neuroscience*, 16:898300, 2022.

[102] Jianliang Min, Ping Wang, and Jianfeng Hu. Driver fatigue detection through multiple entropy fusion analysis in an eeg-based system. *PLoS one*, 12(12):e0188756, 2017.

[103] Nathan J Stevenson, Karoliina Tapani, Leena Lauronen, and Sampsa Vanhatalo. A dataset of neonatal eeg recordings with seizure annotations. *Scientific data*, 6(1):1–8, 2019.

[104] Logan T Trujillo. Mental effort and information-processing costs are inversely related to global brain free energy during visual categorization. *Frontiers in neuroscience*, 13:1292, 2019.

[105] N. Wagh, J. Wei, S. Rawal, et al. Evaluating latent space robustness and uncertainty of eeg-ml models under realistic distribution shifts. *Advances in Neural Information Processing Systems*, 35:21142–21156, 2022.

[106] Ann-Kathrin Kiessner, Robin T Schirrmeister, Joschka Boedecker, and Tonio Ball. Reaching the ceiling? empirical scaling behaviour for deep eeg pathology classification. *Computers in Biology and Medicine*, 178:108681, 2024.

[107] Wikipedia. Event-related potential, 2025. Accessed: 2025-07-30.

[108] Siyuan Zang, Xiaojun Ding, Meihong Wu, and Changle Zhou. An eeg classification-based method for single-trial n170 latency detection and estimation. *Computational and Mathematical Methods in Medicine*, 2022(1):6331956, 2022.

[109] Joaquin Navajas, Maryam Ahmadi, and Rodrigo Quian Quiroga. Uncovering the mechanisms of conscious face perception: a single-trial study of the n170 responses. *Journal of Neuroscience*, 33(4):1337–1343, 2013.

[110] Yin Tian, Huiling Zhang, Yu Pang, and Jinzhao Lin. Classification for single-trial n170 during responding to facial picture with emotion. *Frontiers in computational neuroscience*, 12:68, 2018.

[111] Jiajing Zhao, Mengyi Bao, Wencong Ruan, Rui Kuang, Haifeng Li, Yueming Wang, and Lin Yao. Electrophysiological abnormalities associated with sustained attention in children with attention deficit hyperactivity disorder and autism spectrum disorder. *IEEE Transactions on Neural Systems and Rehabilitation Engineering*, 2025.

[112] Alfonso Mastropietro, Ileana Pirovano, Alessio Marciano, Simone Porcelli, and Giovanna Rizzo. Reliability of mental workload index assessed by eeg with different electrode configurations and signal pre-processing pipelines. *Sensors*, 23(3):1367, 2023.

[113] Winnie KY So, Savio WH Wong, Joseph N Mak, and Rosa HM Chan. An evaluation of mental workload with frontal eeg. *PLoS one*, 12(4):e0174949, 2017.

[114] Wenbin Li, Shan Cheng, Jing Dai, and Yaoming Chang. Effects of mental workload manipulation on electroencephalography spectrum oscillation and microstates in multitasking environments. *Brain and Behavior*, 15(1):e70216, 2025.

[115] Gianluca Di Flumeri, Gianluca Borghini, Pietro Aricò, Nicolina Sciaraffa, Paola Lanzi, Simone Pozzi, Valeria Vignali, Claudio Lantieri, Arianna Bichicchi, Andrea Simone, et al. Eeg-based mental workload neurometric to evaluate the impact of different traffic and road conditions in real driving settings. *Frontiers in human neuroscience*, 12:509, 2018.

[116] KUN-TA CHOU, YU-TIEN CHANG, YUH-MIN CHEN, KANG-CHENG SU, DIANG-WANG PERNG, SHI-CHUAN CHANG, and GUANG-MING SHIAO. The minimum period of polysomnography required to confirm a diagnosis of severe obstructive sleep apnoea. *Respirology*, 16(7):1096–1102, 2011.

[117] Yangxuan Zhou, Sha Zhao, Jiquan Wang, Haiteng Jiang, Zhenghe Yu, Shijian Li, Tao Li, and Gang Pan. Simplifying multimodal with single eog modality for automatic sleep staging. *IEEE Transactions on Neural Systems and Rehabilitation Engineering*, 32:1668–1678, 2024.

[118] Gayal Kuruppu, Neeraj Wagh, and Yogatheesan Varatharajah. Eeg foundation models: A critical review of current progress and future directions, 2025.

[119] Jiamin Wu, Zichen Ren, Junyu Wang, Pengyu Zhu, Yonghao Song, Mianxin Liu, Qihao Zheng, Lei Bai, Wanli Ouyang, and Chunfeng Song. Adabrain-bench: Benchmarking brain foundation models for brain-computer interface applications. *arXiv preprint arXiv:2507.09882*, 2025.

[120] BrainAccess. Eeg foundation models: Unlocking the next generation of neurotechnology, July 2025.

[121] Khaled Saab, Siyi Tang, Mohamed Taha, Christopher Lee-Messer, Christopher Re, and Daniel L Rubin. Towards trustworthy seizure

onset detection using workflow notes. *npj Digital Medicine*, 7(1):42, 2024.

[122] Ashish Jaiswal, Mohammad Zaki Zadeh, Aref Hebri, and Fillia Makedon. Assessing fatigue with multimodal wearable sensors and machine learning. *arXiv preprint arXiv:2205.00287*, 2022.

[123] Limin Wang, Toyotaro Suzumura, and Hiroki Kanezashi. Graph-enhanced eeg foundation model. *arXiv preprint arXiv:2411.19507*, 2024.